Automatic Suppression of Spatially Variant Translational Motion Artifacts in Magnetic Resonance Imaging

Yasser M. Kadah[1,2] and Xiaoping Hu[2]
[1]Biomedical Engineering Department, Cairo University, Giza, Egypt, and
[2]Center for Magnetic Resonance Research, University of Minnesota, Minneapolis MN 55455
E-mail: kadah@geronimo.drad.umn.edu

Abstract

This paper summarizes the theory of a novel post-processing approach to automatic motion artifact suppression in magnetic resonance imaging. The main advantage of the new approach is its treatment of a more practical spatially variant translational motion model that is fundamentally different from previous work in the literature. We first consider a 1-D model for the problem based on differentiated rather than original image. In this model, the motion artifact amounts to blurring of peaks corresponding to the edges in the original image. Observing that the distorted and true images share the same 2-norm, we search for the true image on the hyper-sphere with radius equal to this norm. We show that the solution must have the minimum 1-norm of all vectors on the hyper-sphere and a search strategy based on dynamic programming is used to estimate the motion at a reasonable complexity. Subsequently, this procedure is applied to different regions in the image independently and spatially variant motion model parameters are derived at a resolution of the region sizes. Finally, we show the similarity between this problem and the problem of magnetic field inhomogeneity distortion. Based on this similarity, an image reconstruction strategy and an expression for the point-spread function of the resultant image are derived. The new technique is applied to correct computer simulated images and promising results are obtained.

1 Introduction

Accurate diagnosis in medical procedures has become widely attainable by the advent of the different medical imaging modalities. Among those, magnetic resonance imaging (MRI) is currently one of the most promising non-invasive diagnostic tools in medicine. Besides its ability to produce anatomical images of remarkable detail and contrast, it can also be used to visualize vascular structures, measure blood flow and perfusion, detect neural activation, and identify the metabolic information of different areas in the acquired images. In addition, its inherently volumetric acquisition permits slices at different angles to be computed easily, which can be advantageous in many applications.

One of the main problems in the present magnetic resonance imaging technology is its susceptibility to severe artifacts when motion occurs during the image acquisition period. These artifacts manifest themselves as prominent blurring in the areas where motion occurred. This practically limits the clinical usefulness of such acquisitions and in most cases requires the imaging experiment to be repeated at the expense of decreased patient comfort and inefficient use of the MRI machine. As a result, developing a technique that can boost the tolerance of the present MRI technology to motion can be a major impact on advancing its clinical use even further.

To mathematically understand the origin of motion artifacts, consider a magnetic resonance experiment in which an object of signal magnitude spatial distribution $f(\vec{x})$ is imaged. In this case, the collected data take the form:

$$F(\vec{k}) = \int_{-\infty}^{\infty} f\left(\xi(\vec{k},\vec{x})\right) e^{-j2\pi\vec{k}\cdot\vec{x}}\, d\vec{x}, \qquad (1)$$

where $\xi(\vec{k},\vec{x})$ is a general function that defines the position of the imaged object when the point $\vec{k}$ is collected as a function of the initial position $\vec{x}$. In the ideal case when $\xi(\vec{k},\vec{x}) = \vec{x}$, the true image can be reconstructed using an inverse Fourier transformation. Otherwise, the image reconstruction problem becomes the one of estimating $f(\vec{x})$ given $F(\vec{k})$ without prior knowledge of $\xi(\vec{k},\vec{x})$, which is a far more difficult problem.

1.1 Previous Work

Several methods to solve the problem of motion artifacts in MRI have been reported in the literature (cf.[1] for a fairly comprehensive list of references). In general, the available techniques can be classified into four main categories. The first category attempts to suppress relative patient motion among different k-space lines within a given image through either breath holding and chest strapping, or by using cardiac and respiratory gating. This effectively minimizes the physiological component of motion between these lines at the expense of increased discomfort to the patient and/or significantly longer acquisition times. The second category uses smart averaging of different acquisitions to suppress the motion artifacts besides improving the signal-to-noise ratio of the final image. This

0-8186-8821-1/98 $10.00

works by taking the average of the corresponding k-space lines in a number of consecutive image acquisitions, or more generally by composing a weighted average of them based on optimizing a certain objective function under given constraints. The third category applies extra magnetic gradient lobes in the imaging sequence to eliminate the effects of motion through signal refocusing assuming a simple polynomial model for this motion. This technique is used mainly for minimizing signal loss from moving blood and cerebrospinal fluid within a given voxel. Finally, the fourth category assumes simple forms of global rigid body motion including translational and rotational components and corrects for them in a post-processing step. The motion in this category is estimated using external monitoring, navigator echo, symmetry constraints, motion periodicity constraint, or through automated techniques. These techniques work well for such applications where the global rigid body motion model applies well. However, in many situations, they represent solutions to only a restricted class of artifacts and cannot generally be applied to more complex types of motion encountered in practice such as spatially variant or deformable body motions. Therefore, a motion suppression technique that can be applied for spatially variant motion is likely to have a high potential in clinical applications.

In this paper, we address the problem of motion artifact suppression under a more general spatially-variant translational motion model. First, a 1-D model for the problem based on differentiated rather than original image is developed. In this model, the motion artifact amounts to blurring of peaks corresponding to the edges in the original image. Observing that the distorted and true images share the same 2-norm, a fast dynamic programming search for the true image on the hyper-sphere of possible solutions based on a minimum 1-norm criterion and imposing a simple practicality constraint. Subsequently, this procedure is applied to different regions in the image independently and a spatial-temporal motion map describing the spatially-variant motion model is computed. We show the similarity between the motion artifacts problem and the inhomogeneity distortion problem, and an optimal correction method and the point-spread function of the correction are derived based on this knowledge. The technique is applied to correct computer simulated images and promising results are obtained.

2 Model

Consider the process of imaging a 1-D object $f(x)$ using MRI (without loss of generality). Under the assumption of piecewise constant signal magnitude within individual pixels, it is mathematically possible to express any 1-D magnitude distribution $g(x)$ in terms of a finite summation of shifted unit step functions of different amplitudes in the form [2]:

$$g(x) = \sum_{n=1}^{N} c_n u(x - x_n). \qquad (2)$$

When this model is differentiated with respect to x, the result corresponds to a similar summation of a number of shifted delta-functions representing the edges within the image. This edge distribution is a characteristic feature or a *signature* of each tissue type. Since each of these delta functions has a frequency domain representation in the form of a constant magnitude multiplied by a linear phase, windowed versions of the k-space at different locations contain similar amounts of information about those edges. In other words, given their accurate description of the underlying structures, these edges can be considered as *invariant* signatures of the tissue that can be estimated from any finite-size window in the k-space. In order to derive the tissue signature from the collected k-space data corresponding to the original image, a differentiation step must be performed. This is achieved by multiplying the k-space by a linear function of k, the k-space frequency variable, following the Fourier differentiation theorem such that:

$$f(x) = g'(x) = \mathcal{F}^{-1}\{jkG(k)\} = \sum_{n=1}^{N} c_n \delta(x - x_n). \qquad (3)$$

In MRI, images/volumes are constructed by collecting their k-space representations. The motion artifacts arise from the fact that different k-space points are collected at different instances of time. If the assumption of subject stationarity during the imaging experiment is not closely satisfied, the collected k-space corresponds to an incoherent collection of snapshots of the object at different positions. It should be noted that the differentiation step is a *motion-safe* operation since it does not mix different points in the k-space together to derive the result. Consequently, each point in the k-space of the differentiated image maintains a unique acquisition time exactly like the original k-space.

Given the nature of the data acquisition in MRI, it is reasonable to assume that the relative motion within any localized collection of k-space points is negligible. For example, if we sample an $L \times L$ k-space on a rectangular grid in a row-by-row fashion, it is possible to assume that the relative motion within any consecutive $M < L$ rows is negligible. In this case, the collected k-space is divided into a number of *sub-bands*, each representing a snap-shot of the imaged object within the acquisition period. To illustrate this decomposition, we will consider the one-dimensional case without loss of generality. Any one dimensional signal can be divided into independent segments by windowing in the form:

$$F(k) = \sum_{n=1}^{L} F_n(k) = \sum_{n=1}^{L} F(k) \cdot \sqcap\left(\frac{k - k_i}{\Delta k}\right), \qquad (4)$$

where $\sqcap(\cdot)$ is the gate function, k_i is the center of sub-band i and Δk is the uniform width of the sub-bands. Consequently, the sub-band images $f_i(x)$ obtained as the inverse Fourier transformations of $F_i(k)$ can be expressed as:

$$f_n(k) = f(x) * \left[Sinc(\frac{\Delta k \cdot x}{2}) e^{j2\pi k_n x}\right]. \qquad (5)$$

In other words, the sum of delta-functions in (3) is converted to an equivalent sum of orthogonal functions of more general form.

Applying the same concept of localization in the spatial domain, we realize that by windowing the spatial domain of the object, a dual-domain localized cells can be derived for the above example in the form:

$$f_{n,m}(k) = \left(f(x) * \left[Sinc(\frac{\Delta k \cdot x}{2}) e^{j2\pi k_n x} \right] \right) \cdot \sqcap \left(\frac{x - x_m}{\Delta x} \right). \quad (6)$$

Each of these spatial-temporal cells maintains orthogonality with all other cells. At the same time, each represents a snapshot of a part of the image during a brief period within the image acquisition time. Therefore, by estimating the relative motion within each of these different parts along the acquisition time line, a temporal-spatial motion map for the object during the the imaging experiment can be derived and corrected for.

3 Motion Estimation

In order to derive a criterion for estimating relative motion between spatial-temporal cells, consider first the effect of motion on one of these cells. Based on Eqn.(1), the effect of translational rigid-body motion on different sub-bands can be shown to be a multiplication by a phase term that is determined by the amount of motion in the form:

$$F_{n,m}(k) = \int f_{n,m}(x - \Delta(n,m)) e^{-j2\pi kx} dx$$
$$= e^{j2\pi k \cdot \Delta(n,m)} \int f_{n,m}(x) e^{-j2\pi kx} dx, \quad (7)$$

where $\Delta(n,m)$ is the displacement of spatial-temporal cell $F_{n,m}$ as a result of its translational motion. Hence, the problem of automatic translational motion correction becomes the one of estimating and compensating for these phase terms. The effect of these phase terms is to cause the different spectral components of a given edge to misalign resulting in a blurred reconstruction. Therefore, a suitable objective function in the search for the optimal values of the phase functions should be sensitive to this blurring.

From the problem formulation stated in Eqn.(7), we observe the following identity:

$$||F_d(k)||_2^2 = \int F_d(k) \cdot F_d^*(k)\, dk = ||f(x)||_2^2 = \eta^2, \quad (8)$$

where $F_d(.)$ is the Fourier transform of the motion-distorted image, $f(x)$ is the original image, and η is a positive real value and can be shown to be constant with respect to the translational motion Δx. This identity follows directly from the definition of the 2-norm and from Parseval's identity of the Fourier transform [3]. Hence, the phase factor in Eqn.(7) does not affect the 2-norm of the resultant image. Consequently, the solution for our reconstruction problem is within a set of vectors lying on the surface of a hypersphere of radius η. To illustrate this with an example, consider a 1-D image containing a single edge represented by a single non-zero value taken to be the unity in the derivative image vector. The effect of motion appears as derivative image vector with at least two non-zero entries corresponding to the resultant smearing of the edge. The distorted and undistorted vectors share a common 2-norm of unity.

Hence, the solution strategy should seek to focus the different sub-band components, $f_{i,j}(x), \forall i$, of the different edges within the derivative image of interest by properly shifting each by $\Delta \hat{x}_i$ (or phasing them in k-space) to realign. In other words, the phase factors should be chosen such that the sum of all sub-band components of an edge either yields the most zero entries (minimum 1-norm), or contain the largest value of any single entry in the solution vector (maximum ∞-norm). In a mathematical form, the first focusing criterion can be expressed as:

$$\min_{\Delta \hat{x}_n} \left\{ ||f_c(x)||_1 = \sum_x \left| \sum_n f_{n,m}(x - \Delta \hat{x}_n) \right| \right\},$$
$$Subject\ to\ \ ||f_c(x)||_2 = \eta. \quad (9)$$

These norms change substantially when the phase values of Eqn.(7) change and their respective minimum and maximum points correspond to the desired solution. For example, in the 2-D case without loss of generality, the circles defined by $||f||_1 = 1$, $||f||_2 = 1$, and $||f||_\infty = 1$ intersect only on the axes. Any point in $\mathcal{R}^2$ satisfies the condition $||f||_1 \geq ||f||_2 \geq ||f||_\infty$ and the equality happens only when only one of the entries of the vector is nonzero. In other words, the desired solution is represented by one of the four unit vectors that lie along one of the axes in either direction. In the general case, any of the possible solutions may differ by only a change of sign or a simple shift with respect to the true solution. Even though either of these two effects is usually considered unimportant and can be easily accounted for in simple cases, this is not true for the general case where more than one edge exists or when the translational motion is space variant. As a result, two constraints are imposed in order to obtain a unique solution. The first constraint is the positive definiteness of the solution, imposed by the nature of the physical objects imaged by MRI which may only have positive spin densities. The remaining solution resulting from shifting the unique solution by different amounts can be eliminated by another constraint imposed from an assumption that the imaged subject was still at the beginning of the data acquisition period (or equivalently, referencing the solution to F_{00}).

For the general case of clinical MRI, it is expected to have many edges within any given region in the image and noisy data collection is expected. Under these conditions, the ∞-norm criterion is more prone to errors because of its dependence on the value of a single entry in the solution vector that might not reflect the true nature of the entire solution. As a result, due to the robustness against such errors, the 1-

norm criterion in Eqn.(9) is selected to be the focusing objective function of choice for this work.

Now consider the spatially variant case of interest where several spatial-temporal cells are considered. Under the assumption that motion within spatial cells in the image plane can be sufficiently described by a rigid body translational motion model, the above procedure can be applied to different overlapping/non-overlapping cells to derive the motion parameters for different regions by computing the local focusing norm for each independently. Hence, a spatial-temporal map of the motion is computed during this procedure that accounts for not only the time-variability of the motion, but also for possible spatial variability at any given time. The image is subsequently reconstructed by concatenating its corrected pieces.

4 Correction Point Spread Function

In order to obtain the point spread function of the correction using this method, we derive a similarity between the motion correction problem and the magnetic field inhomogeneity distortion problem. Once the spatial-temporal motion map $\Delta(i,j)$ is computed at a particular resolution, it is interpolated in the spatial domain to derive a motion map $\Delta(x,k)$ with full spatial resolution under the assumption of smooth motion distribution. Invoking the assumption of spatially-variant translational motion to the 1-D form of Eqn.[1] such that $\xi(k,x) = x + \Delta(x,k)$, the detected k-space becomes:

$$F_d(k) = \int f(x+\Delta) e^{-j2\pi kx}\ dx. \tag{10}$$

Define $y = x + \Delta$. Then, $dy = dx \cdot (1 + \frac{\partial\Delta(x,k)}{\partial x} + \frac{\partial\Delta(x,k)}{\partial k}\frac{dk}{dx})$. Since x and k are independent, the derivative $\frac{dk}{dx}$ is zero. Hence, the k-space equation takes the form:

$$F_d(k) = \int f(y) e^{-j2\pi k(y-\Delta)} \left(1 + \frac{\partial \Delta}{\partial x}\right)_{x=(y-\Delta)} dy. \tag{11}$$

Note that the term $(1 + \frac{\partial\Delta(x,k)}{\partial x})$ is the Jacobian term that accounts for intensity changes as a result of compression/dilation of the different parts of the image. Under the assumption of rigid-body motion (albeit spatially variant still), this term has to become unity. In this case, the problem can be conveniently reformulated as:

$$F_d(k) = \int f(y) e^{j2\pi j\Delta(k,y)} e^{-j2\pi ky} dy. \tag{12}$$

We observe that the motion in this formulation manifests itself as a phase distortion to an ideal stationary object. In other words, since the spatial domain is encoded by linear gradients that effectively assign unique resonance frequencies to different spatial locations, the moving parts of the object acquire an additional motion-dependent phase as a result of being at a different resonance frequency at the time of data collection. We observe that Eqn.[12] is similar to the equation of the data collected under magnetic field inhomogeneity, with the main difference being the separability of the spatial and spatial frequency parts of the distortion phase term in the inhomogeneity distortion whereas it is not in the motion distortion. This is a direct result of the fact that the phase progression in the inhomogeneity correction problem is linear in time by its nature, while it is of a rather arbitrary form in the motion distortion problem. From the theoretical derivation for the inhomogeneity distortion problem in [5], it is straightforward to propose an equivalent solution for the motion distortion problem in the form:

$$F_c(k) = \int f_d(y) e^{-j2\pi j\hat{\Delta}(k,y)} e^{-j2\pi ky} dy, \tag{13}$$

where $F_c(k)$ is the corrected k-space, f_d is the distorted image, and $\hat{\Delta}(y,k)$ is the estimated translational motion map of the spatial position y when the k-space line k was collected. Similarly, the point spread function of this solution takes the form:

$$PSF(y, y_o, \Delta(i,j) - \hat{\Delta}(k,y)) = \sum_i e^{-j2\pi j(\Delta(i,j)-\hat{\Delta}(i,j))} e^{-j2\pi k(y-y_o)}. \tag{14}$$

This indicates that perfect correction is possible given an accurate estimate of the spatial-temporal motion map. It should be noted that the solution obtained by phasing the k-space cells can equivalently be derived based on the conjugate phase technique [4]. However, the implementation using the Fourier shift theorem in ?? might be advantageous in many cases for more uniform correction results.

5 Results and Discussion

In order to verify the theory, the proposed method was implemented to correct different computer simulated 1-D profiles as well as images of the Shepp-Logan phantom with spatially variant amounts of translational motion. In Fig.(1), a 256-point 1-D model consisting of bands bright bands on a dark background is considered. The white bands move independently along time with a time step equivalent to two k-space lines. The motion artifacts due to this motion are clear in the left image. The spatially-variant motion was estimated and corrected for and the results appear in the middle image. Compared to the original image to the right, a substantial improvement in the corrected image can be observed. In Fig.(2), the true (dashed line) and estimated (solid line) motion trajectories for one of the band are plotted. As can be observed, the estimated motion adheres closely to the true motion trajectories. The average absolute deviation of the two trajectories was 0.52 pixels and therefore the point-spread function is expected to be very close to an ideal delta-function. This explains the excellent qualitative results obtained in this case. In Fig.(3), a 2-D example is presented where four independently-moving Shepp-Logan phantoms were simulated inside a stationary box of uniform intensity. The motion-corrupted image on the left was corrected to the image on the right.

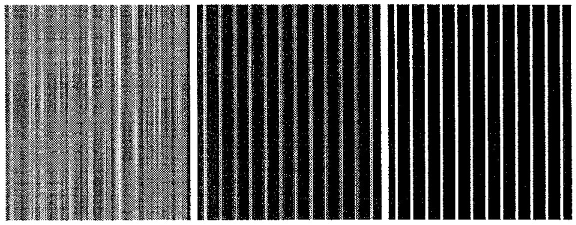

Figure 1: 1-D correction example.

The k-space here was divided into 16 non-overlapping, uniform cells and the image was divided into 16 square cells in the 256x256 matrix image.

Even though the computation of the 1-norm has a complexity of $O(N)$ flops, there is still a concern about the complexity of the whole multiple optimization procedures involved in the proposed method and its practicality. The problem requires the estimation of the values of M variables, each may assume any value from a set of L possible values. That is, the search space has a huge size of L^M entries and does not maintain convexity. In order to solve this problem at the smallest cost, a dynamic programming procedure was used to compute the solution at any desired resolution, which amounts to a substantially lower number of search operations of $L \cdot M$. As a result, the total complexity of the proposed method is $O(L \cdot M \cdot N_r^2)$ flops per region (where N_r is the region size). Therefore, the proposed method is possible to implement at a fairly reasonable computational cost.

Based on the results from the computer simulations, the clinical potential of the proposed technique appears to be rather significant. The potential benefits of this technique include efficient data acquisition of MR images, which translates into more cost-effective use of MR machines in addition to increased comfort to the patient. Examples of possible applications include abdominal imaging where spatially varying motion is encountered and the proposed technique can be used with fast spin echo sequences without need for respiratory gating or breath holding. Also with the rapid growth of interventional MRI, the proposed method can be adapted to provide additional freedom to the surgeon. Further work is needed to explore the true potential of the new method in clinical practice.

6 Conclusions

A novel post-processing approach for automatic motion artifact suppression in magnetic resonance imaging was developed. The new approach treats a more general spatially-variant translational motion model that is fundamentally different from previous methods. The theory of the new technique was developed and verified by computer simulations. Further work is needed to explore the clinical potential of this work.

Acknowledgments

This work was supported by grants RR08079 and MH55346 from NIH.

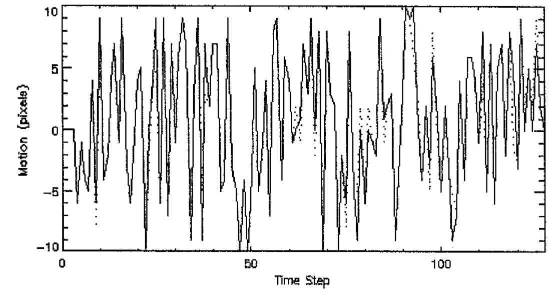

Figure 2: Example of estimated and true motion trajectories

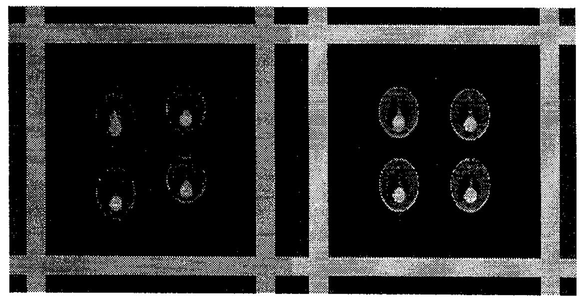

Figure 3: 2-D correction example.

References

[1] R.A. Zoroofi, Y. Sato, S. Tamura, and H. Naito, "MRI artifact cancellation due to rigid motion in the imaging plane," *IEEE Trans. Med. Imag.*, vol. 15, no. 6, pp. 768-784, 1996.

[2] E.M. Haacke, Z.-P. Liang, and S.H. Izen, "Superresolution reconstruction through object modeling and parameter estimation," *IEEE Trans. Sig. Proc.*, vol. 37, no. 4, pp. 592-595, 1989.

[3] D.S. Watkins, *Fundamentals of Matrix Computations*, John Wiley & Sons, New York, 1991.

[4] A. Maeda, K. Sano, T. Yokoyama, "Reconstruction by weighted correlation for MRI with time-varying gradients," *IEEE Trans. Med. Imag.*, vol. 7, pp. 26-31, 1988.

[5] Y.M. Kadah and X. Hu, "Simulated phase evolution rewinding (SPHERE): a technique for reducing B_0 inhomogeneity effects in MR images," Magn. Res. Med., vol. 38, no. 4, pp. 615-627, 1997.